Parity Relations for Linear Uncertain Dynamic Systems

Stéphane M. Ploix [a] Olivier Adrot [a]

[a] *Laboratoire d'Automatique de Grenoble, INPG, UJF, UMR 5528, BP 46, F-38402 Saint Martin d'Hères Cedex, France*

Abstract

A new approach for the design of parity relations for linear dynamic systems with additive and multiplicative uncertainties is presented. Instead of canceling uncertainties following the example of the so-called robust approaches, uncertain parity relations take uncertainties into account as bounded variables. The method is based on the analysis of zonotopes representing the uncertainties. It leads both to Boolean detection results and to an indicator representing the distance to the opposite decision.

Key words: fault detection, uncertain dynamic linear models, set-membership approach

1 Introduction

Many works in the international literature, for the past 15 years, have dealt with diagnosis of physical systems. Most of the works developed within the Automatic Control community focus on fault detection. Several detection tools have emerged: state observer based residuals generators, parity relations and parameter estimation based detection approaches are the main trends. This paper focuses on parity relations, which have been introduced by [4], and improved by [9]. These techniques are indeed particularly relevant for fault diagnosis because they lead to very short time windows, which reduce the detection time. They are also very general techniques: the equivalence between the results provided by parity relations and state observer based approaches has been demonstrated in [19]. Although these techniques are well-suited for deterministic models, they attempt to cancel uncertainties without taking them into consideration during detection in uncertain context [13]. The Kalman filter is an exception here, because it includes vectors of stochastic variables and helps to automatically determine thresholds indexed on standard deviations. Unfortunately, the uncertainties appearing in the models used by Kalman filters are additive, which can only converge to regular thresholds around variables reconstructed by the filter. Only few researchers have shown an interest in techniques taking multiplicative uncertainties into consideration. Let's cite [8], which has proposed a method based on the Pontryagin principle to estimate the enclosures of uncertain systems.

About fifteen years ago, many studies formulating identification problems within a set-membership context have appeared [11,18,21]. Instead of representing the uncertainties by means of Gaussian stochastic variables, these approaches, known as bounding approaches or set-membership approaches, represent the uncertainties by a set of possible values of which only the bounds are known. These works have been summarized in [10]. Since 1995, researchers have been interested in taking into account modelling uncertainties in fault detection [?,?,?]. Set-membership approaches of fault detection based on the Hansen algorithm in [6,7] and on the worst-case simulation have been proposed in [16]. However, approaches based on Pontryagin principle, on Hansen algorithm or on the worst-case simulation require lots of computations at each sample time, which are generally incompatible with real-time constraint in complex dynamic systems.

In parallel, diagnostic analysis, also called isolation, has evolved. [17] and [5] have proposed a logically sound diagnostic analysis. These works only apply to deterministic static systems, but their considerable interest resides in the fact that they formulate the diagnostic problem in a very formal way, in particular by introducing the concept of consistency. Recently, new isolation approaches have been developed [12,15]. They aim at merging the accuracy of the detection tools provided by the Automatic Control community with the logically sound diagnostic analysis provided by the Artificial Intelligence community. These new results are able to guarantee the diag-

Email addresses: stephane.ploix@inpg.fr (Stéphane M. Ploix), olivier.adrot@inpg.fr (Olivier Adrot).

nostic analysis step i.e. if the symptoms provided by the detection tests are true, then all the possible diagnoses are found and one of them corresponds to the actual system state. However, in the very common uncertain context, deterministic detection tests neglect uncertainties and therefore, they cannot guarantee their symptoms. Guaranteed detection tests for dynamic systems modelled by differential equation containing uncertainties is henceforth a main issue.

Having this in mind, it now remains to take a look at what a detection test becomes when the behavioural model contains uncertainties. In the case of deterministic models, it is enough to check whether the observations in turn satisfy the models' deterministic equations. What happens in an uncertain context? First and foremost, an uncertain model represents a set of possible behaviours. This set may be represented by distribution laws as in the Kalman filtering in the stochastic framework. Although Kalman filter applies to various laws, distribution laws of estimated sets, which have to be known for detection purposes, cannot be deduced from computed expectations and variances. Indeed, if the Gaussian distributions remain Gaussian for addition, they no longer are for multiplication. As far as the laws of uniform distribution are concerned, these are already not stable for addition. Otherwise put, if the Gaussian stochastic variables are particularly suitable for the representation of additive structures of uncertainties, Gaussian distributions are unsuitable for multiplicative uncertainties. In order to tackle models containing uncertainties by a bounding approach, the concept of membership value set is introduced, given as $\mathcal{M}(\ )$, by analogy with the stochastic variables. If X is a bounded variable, in other words, if it is only known by the set to which it belongs, then this set will be given as $\mathcal{M}(X)$. The notation x should designate a particular realization of X; nevertheless, for the sake of simplicity, the notation of a realization x will be merged with that of the bounded variable X itself. Henceforth, x will designate, alternately, the bounded variable and one of its realizations, and $\mathcal{M}(x)$ will designate the membership value set of the bounded variable. State space models containing multiplicative and additive uncertain parameters are studied in this paper. It should be noted that by uncertain it is meant that uncertain parameters correspond to time varying variables, of which only the bounds are known. Even if it contains less information than stochastic approaches, the set-membership approach in fault detection has wider application and provides exactly the required information in describing the set of all the possible behaviours by its bounds only. The question to be answered is indeed: are the observations consistent with one of the possible behaviours or not?

After stating the problem in section 2, section 3 proposes an algorithm to compute uncertain parity relations and section 4 shows how to use uncertain parity relations to compute detection decisions in the form of a set of inequalities to be satisfied. Finally, section 5 presents an application example. It points out that uncertain parity relations may lead to more precise decisions than deterministic parity relations in reducing misdetections.

2 Problem statement

When considering uncertainties, it is necessary to distinguish between two kinds of variables: unknown physical variables and known values such as measured or controlled values, which are topped by a "~". For instance, the following relation can represent the behaviour of a sensor: $\tilde{y} = (1 + \upsilon)y$ where υ represents an uncertain parameter, y the physical variable and $\tilde{y}$ the measured value of y. For the sake of simplicity, uncertainties will be represented by normalized independent bounded variables, of which the membership value set is equal to [-1,1]. For instance, a parameter υ whose value belongs to [2,6], will be written $\upsilon = 4 + 2\theta$ where θ is a normalized uncertain variable: $\mathcal{M}(\theta) = [-1, 1]$.

Consider the following general uncertain linear state space model, function of $q_1 + q_2$ uncertain bounded variables:

$$\begin{cases} \frac{dx}{dt} & = \underline{A}(\vartheta, \theta)x + \underline{B}(\vartheta, \theta)\tilde{u} \\ \tilde{y} & = \underline{C}(\vartheta, \theta)x + \underline{D}(\vartheta, \theta)\tilde{u} \end{cases} \tag{1}$$

where $(\vartheta, \theta)/\|[\vartheta^\top, \theta(t)^\top]^\top\|_\infty \leq 1$, $x \in \mathbb{R}^n$, $\tilde{y} \in \mathbb{R}^p$, $\tilde{u} \in \mathbb{R}^m$, $\vartheta \in \mathbb{R}^{q_1}$, $\theta(t) \in \mathbb{R}^{q_2}$ and $\tilde{u} = \tilde{u}(t)$, $x = x(t)$, $y = y(t)$, $\theta = \theta(t)$.

Contrary to uncertain variables in θ, uncertain variables gathered in ϑ are partially known but invariant. Because parity relations induce finite time horizons, it is quite usual to consider that some bounded variables are time-invariant over the considered horizon.

Assuming that $\tilde{u}$ and θ do not vary over a sampling period $[kT_e, (k + 1)T_e]$, a discrete-time model, where matrices have been linearized with respect to uncertain variables, can be found (see Appendix):

$$\begin{cases} x_{k+1} & = A_k x_k + B_k \tilde{u}_k \\ \tilde{y}_k & = C_k x_k + D_k \tilde{u}_k \end{cases} \tag{2}$$

with $x_k = x(kT_e)$, $\tilde{y}_k = \tilde{y}(kT_e)$, $\tilde{u}_k = \tilde{u}(kT_e)$, $\theta_k = \theta(kT_e)$ and

$$\begin{aligned} A_k &= A_0 + \textstyle\sum_{i=1}^{q_1} A_i \times (\vartheta)_i + \sum_{i=1}^{q_2} A_{q_1+i} \times (\theta_k)_i \\ B_k &= B_0 + \textstyle\sum_{i=1}^{q_1} B_i \times (\vartheta)_i + \sum_{i=1}^{q_2} B_{q_1+i} \times (\theta_k)_i \\ C_k &= C_0 + \textstyle\sum_{i=1}^{q_1} C_i \times (\vartheta)_i + \sum_{i=1}^{q_2} C_{q_1+i} \times (\theta_k)_i \\ D_k &= D_0 + \textstyle\sum_{i=1}^{q_1} D_i \times (\vartheta)_i + \sum_{i=1}^{q_2} D_{q_1+i} \times (\theta_k)_i \end{aligned}$$

Remark 1 *The bounded variables θ_k are considered as independent time-varying variables. Consequently,* *at two different times k_1 and k_2, the same uncertain variable $(\theta_k)_i$, standing for the i^{th} component of θ_k, is represented by two independent bounded variables $(\theta_{k_1})_i$ and $(\theta_{k_2})_i$ whose membership value sets are identical: $\mathcal{M}((\theta_{k_1})_i) = \mathcal{M}((\theta_{k_2})_i)$.*

Residuals generators are usually based on state observers. However, in a set-membership context, except for some particular cases, the recurrence leads to replace state space value sets by simpler outer value sets, such as boxes or ellipsoids, that yields some over-estimations. Propagating these approximations induces an accumulation of errors leading to an explosion of computed sets, usually called wrapping effect [2,3]. Checking on a finite horizon, such as parity relations do, avoids this drawback because integration over an long time window is not required. Then, the detection problem amounts to check if a set of known values $\{\tilde{u}_k, \ldots, \tilde{u}_{k+h-1}, \tilde{y}_k, \ldots, \tilde{y}_{k+h-1}\}$ over an horizon $h \in \mathbb{N}^*$ is consistent with model (2).

Considering model (2) and stacking relationships between known values over a time horizon hT_e such as in most of parity relation design approaches [4], the following relationship arises:

$$0 = \begin{bmatrix} \tilde{y}_k \\ \tilde{y}_{k+1} \\ \vdots \\ \tilde{y}_{k+h-1} \end{bmatrix} - \mathcal{O}_h(\upsilon_k)x_k - \Gamma_h(\upsilon_k) \begin{bmatrix} \tilde{u}_k \\ \tilde{u}_{k+1} \\ \vdots \\ \tilde{u}_{k+h-1} \end{bmatrix} \quad (3)$$

with:

$$\upsilon_k = \begin{bmatrix} \vartheta \\ \theta_k \\ \vdots \\ \theta_{k+h-1} \end{bmatrix}, \mathcal{O}_h(\upsilon_k) = \begin{bmatrix} \mathfrak{O}_k^0 \\ \mathfrak{O}_k^{0,1} \\ \vdots \\ \mathfrak{O}_k^{0,h-1} \end{bmatrix}$$

$$\Gamma_h(\upsilon_k) = \begin{bmatrix} D_k & 0 & \ldots & 0 \\ \mathfrak{O}_k^1 B_k & D_{k+1} & & \vdots \\ \vdots & & \ddots & 0 \\ \mathfrak{O}_k^{1,h-1} B_k & \mathfrak{O}_k^{2,h-1} B_{k+1} & \ldots & D_{k+h-1} \end{bmatrix}$$

$$\mathfrak{O}_k^{i,j} = \begin{cases} j > i, & \mathfrak{O}_k^{i,j} = C_{k+j}A_{k+j-1}\ldots A_{k+i} \\ i = j, & \mathfrak{O}_k^{i,j} = \mathfrak{O}_k^i = C_{k+i} \end{cases}$$
$$\forall j \in \{1, \ldots, q_1 + hq_2\}, \mathcal{M}((\upsilon_k)_j) = [-1, 1]$$

The detection problem amounts to determining whether there exists (x_k, υ_k) satisfying (3) . The result depends on the determination of a relevant horizon h. If this horizon is too small, problem may admit a solution even if there are faults. If the horizon is too large, the amount of computations will increase without any benefits. The right determination of h is a key issue.

Definition 2 *An uncertain system defined by (2) is called regularly observable if, for all $h \in \mathbb{N}^+$, the rank of its observable subspaces $\mathcal{O}_h(\upsilon)$ is independent of the uncertainties.*

Assuming the system (2) is regularly observable, the method provided by the deterministic theory [9] may be used to determine the horizon h. For the sake of simplicity, only full row rank matrices C_k from (2) are considered [1] i.e. there are as many parity relations as number of measurements [9]. Under this assumption, system (2) satisfies:

$$\exists h / rank(\Omega(\upsilon_k)) \geq p \quad (4)$$

The dimension of $\Omega(\upsilon_k)$ is assumed to be equal to p. If more parity relations are obtained, only p of them have to be considered.

3 Computing uncertain parity relations

Uncertain model (3) contains three kinds of information: deterministic parameters, partially known parameters, which are modeled by bounded variables, and unknown state vector x_k. Contrary to known and partially known parameters, unknown data cannot be managed. Therefore, this section shows how to cancel unknown state vector with a suitable projection.

If condition (4) is satisfied, it is possible to calculate a projection matrix $\Omega(\upsilon_k)$ satisfying:

$$\forall \upsilon_k / \|\upsilon_k\|_\infty \leq 1, \; \Omega(\upsilon_k)\mathcal{O}_h(\upsilon_k) = 0 \quad (5)$$

The best choice for horizon corresponds to the smallest h satisfying (4) and (5). Equation (3) can be projected with respect to $\Omega(\upsilon_k)$ in order to cancel unknown variables gathered in x_k:

$$0 = \Omega(\upsilon_k) \begin{bmatrix} \tilde{y}_k \\ \tilde{y}_{k+1} \\ \vdots \\ \tilde{y}_{k+h-1} \end{bmatrix} - \Omega(\upsilon_k)\Gamma_h(\upsilon_k) \begin{bmatrix} \tilde{u}_k \\ \tilde{u}_{k+1} \\ \vdots \\ \tilde{u}_{k+h-1} \end{bmatrix} \quad (6)$$

A solution $\Omega(\upsilon_k)$ solving (5) can be numerically computed as detailed below.

[1] Model reductions may be required in order to get a non redundant matrix

Following definitions assume that θ is a s-dimensional vector of uncertain normalized variables such as $\theta = [\,(\theta)_1 \;\dots\; (\theta)_s\,]^\top$ and that ∇ is a vector of $(\mathbb{N}^+)^s$ such as $\nabla = [\,(\nabla)_1 \;\dots\; (\nabla)_s\,]^\top$

Definition 3 *The power-product $\theta_{[\nabla]}$ is defined by: $\theta_{[\nabla]} = (\theta)_1^{(\nabla)_1} \dots (\theta)_s^{(\nabla)_s}$.*

Definition 4 *The order of a power-product $\theta_{[\nabla]}$ is defined by: $\rho(\theta_{[\nabla]}) = \sum_{i=1}^{s} (\nabla)_i$.*

Definition 5 *An uncertain matrix $M(\theta)$ is polynomial if it can be decomposed as $M(\theta) = \sum_{\nabla_i \in \mathcal{V}} M_{[\nabla_i]} \theta_{[\nabla_i]}, \mathcal{V} \subset (\mathbb{N}^+)^s$, where $M_{[\nabla_i]}$ are certain matrices. The set $\mathcal{V}$ is given by function $\pi(.)$: $\pi(M(\theta)) = \mathcal{V}$.*

Definition 6 *The order of an uncertain polynomial matrix $M(\theta)$ is equal to: $\rho(M(\theta)) = \underset{\nabla \in \pi(M(\theta))}{max} \big(\rho(\theta_{[\nabla]})\big)$.*

Because the matrices of the discrete-time state space model (2) result from a linearization, any observability matrix $\mathcal{O}_h(\upsilon_k)$, defined over an horizon h, affine in the uncertain variables, is an uncertain polynomial matrix defined by:

$$\exists \mathcal{V} \subset (\mathbb{N}^+)^{q_1+hq_2} / \mathcal{O}_h(\upsilon_k) = \sum_{\nabla_i \in \mathcal{V}} O_{[\nabla_i]} \upsilon_{k[\nabla_i]} \qquad (7)$$

where $O_{[\nabla_i]}$ are certain matrices such that $dim(\mathcal{O}_h(\upsilon_k)) = dim(O_{[\nabla_i]})$.

Matrix $\Omega(\upsilon_k)$ can be chosen as an uncertain polynomial matrix:

$$\Omega(\upsilon_k) = \sum_{\varpi_i \in \mathcal{W}} \Omega_{[\varpi_i]} \upsilon_{k[\varpi_i]}, \varpi \subset (\mathbb{N}^+)^{q_1+hq_2} \qquad (8)$$

where $\Omega_{[\varpi_i]}$ are certain matrices such that $dim(\Omega(\upsilon_k)) = dim(\Omega_{[\varpi_i]})$.

Proposition 7 *When certain matrices $\Omega_{[\varpi_j]}$ and $O_{[\nabla_i]}$ satisfy respectively (7) and (8), condition (5) becomes:*

$$\forall \sigma \in (\mathbb{N}^+)^{q_1+hq_2}, \sum_{(\nabla_i, \varpi_j) \in \Upsilon_\sigma(\mathcal{O}_h(\upsilon_k))} \Omega_{[\varpi_j]} O_{[\nabla_i]} = 0 \qquad (9)$$

$$\Upsilon_\sigma(\mathcal{O}_h(\upsilon_k)) = \left\{ \begin{array}{l} (\nabla_i, \varpi_j) \in \big(\pi(\mathcal{O}_h(\upsilon_k)) \times (\mathbb{N}^+)^{q_1+hq_2}\big) / \\ \dots \nabla_i + \varpi_j = \sigma \end{array} \right\}$$

PROOF. According to (7) and (8), constraint (5) may be reformulated as:

$$\forall \upsilon_k / \|\upsilon_k\|_\infty \leq 1, \\ \sum_{\varpi_j \in \pi(\Omega(\upsilon_k))} \sum_{\nabla_i \in \pi(\mathcal{O}_h(\upsilon_k))} \Omega_{[\varpi_j]} O_{[\nabla_i]} \upsilon_{k[\nabla_i + \varpi_j]} = 0$$

Because each power-product $\nabla_i + \varpi_j$ cannot be cancelled by another, the sum of all terms containing $\upsilon_{k[\nabla_i+\varpi_j]}$ has to be equal to 0 whatever the value of υ_k is in its value set. From this result arises the proposition 7.

Remark 8 *For a given vector σ, it is easy to compute the set $\Upsilon_\sigma(\mathcal{O}_h(\upsilon_k))$. It corresponds to $\{(\nabla_i, \varpi_j)/\varpi_j = \sigma - \nabla_i, \nabla_i \in \pi(\mathcal{O}_h(\upsilon_k)), (\varpi_j)_l \geq 0\}$.*

Searching for $\Omega(\upsilon_k)$ satisfying (5) is done iteratively by increasing the order $r = \rho(\Omega(\upsilon_k))$ of the sought solution. This order is initially set to $r = 0$. Then, for order r, the power-products appearing in $\Omega(\upsilon_k)\mathcal{O}_h(\upsilon_k)$ are listed. The set of all vectors σ that has to be considered at order $r + \rho(\mathcal{O}_h(\upsilon_k))$ is given by:

$$\Xi^{q_1+hq_2}_{r+\rho(\mathcal{O}_h(\upsilon_k))} = \left\{ \begin{array}{l} \sigma \in (\mathbb{N}^+)^{q_1+hq_2} / \dots \\ \sum_{l=1}^{q_1+hq_2} (\sigma)_l \leq r + \rho(\mathcal{O}_h(\upsilon_k)) \end{array} \right\} \qquad (10)$$

Remark 9 *The set $\Xi^{q_1+hq_2}_{r+\rho(\mathcal{O}_h(\upsilon_k))}$ can be easily computed by developing level by level a search tree where nodes are vectors ϖ_j and each edge corresponds to an uncertain variable of which the exponent is incremented. The size of the tree is equal to $(q_1 + hq_2)^r$.*

Therefore, at order r, a solution matrix $\Omega(\upsilon_k)$, satisfying (9), is sought [2] only when $\sigma \in \Xi^{q_1+hq_2}_r$. According to (4), if the number of solutions is inferior to p, the order r is incremented by 1 and a new global solution $\Omega(\upsilon_k)$ is sought for the new order r.

Because membership value sets modeled by zonotopes [3] are sought, affine solutions for $\Omega(\upsilon_k)$ are required. Nevertheless, terms of order 0 and 1 of the Mac Laurin series of $\Omega(\upsilon_k)$ solving equation (5) cannot be computed without computing the complete solution $\Omega(\upsilon_k)$ i.e. the complete Mac Laurin series.

Definition 10 *A canonical vector e_i^s is a sparse vector of $\mathbb{R}^s$ satisfying:*

$$\forall i \in \{1, \dots, s\}, \forall j \in \{1, \dots, s\}, \begin{cases} (e_i^s)_j = 1 & if\; i = j \\ (e_i^s)_j = 0 & if\; i \neq j \end{cases}$$

When a solution matrix $\Omega(\upsilon_k)$ has been found, it has to be linearized as much as matrix $\Gamma_h(\upsilon_k)$ i.e. only the power-products of which maximum order is lower than 2, are kept. Denoting $\Omega_0 = \Omega_{[0\dots0]^\top}$, $\Omega_i = \Omega_{[e_i^{q_1+hq_2}]}$ and $\Gamma_h(\upsilon_k) = \Gamma_0 + \sum_{i=1}^{q_1+hq_2} (\Gamma_i \times (\upsilon_k)_i) + \circ(\upsilon_k^\top \upsilon_k)$ where

[2] For instance, the constraints can be gathered into a large matrix of which kernel is computed, see example in section 5

[3] A zonotope is a linear transformation of a box

$(\upsilon_k)_i$ stands for the i^{th} element of vector υ_k, the exact parity relation (6) is linearized:

$$0 = \left(\Omega_0 + \sum_{i=1}^{q_1+hq_2} \Omega_i \times (\upsilon_k)_i\right) \begin{bmatrix} \tilde{y}_k \\ \tilde{y}_{k+1} \\ \vdots \\ \tilde{y}_{k+h-1} \end{bmatrix} \dots \tag{11}$$

$$-(\Omega_0\Gamma_0 + \sum_{i=1}^{q_1+hq_2} (\Omega_i\Gamma_0 + \Omega_0\Gamma_i) \times (\upsilon_k)_i) \begin{bmatrix} \tilde{u}_k \\ \tilde{u}_{k+1} \\ \vdots \\ \tilde{u}_{k+h-1} \end{bmatrix}$$

$$\dots + \circ(\upsilon_k^\top \upsilon_k)$$

4 Using uncertain parity relations

Parity relations affine in the uncertainties have been obtained in (11). The way of checking these parity relations has now to be presented. A method used for static uncertain system presented in [14] has been adapted. Relation (11) can be reformulated in collecting uncertain variables:

$$0 = N_k + M_k\upsilon_k + \circ(\upsilon_k^\top \upsilon_k) \tag{12}$$

$$N_k = \Omega_0 \begin{bmatrix} \tilde{y}_k \\ \vdots \\ \tilde{y}_{k+h-1} \end{bmatrix} - \Omega_0\Gamma_0 \begin{bmatrix} \tilde{u}_k \\ \vdots \\ \tilde{u}_{k+h-1} \end{bmatrix}$$

$$M_k = \dots$$

$$\begin{bmatrix} \dots\ \Omega_i \begin{bmatrix} \tilde{y}_k \\ \vdots \\ \tilde{y}_{k+h-1} \end{bmatrix} - (\Omega_i\Gamma_0 + \Omega_0\Gamma_i) \begin{bmatrix} \tilde{u}_k \\ \vdots \\ \tilde{u}_{k+h-1} \end{bmatrix} \dots \end{bmatrix}$$

where only column corresponding to $(\upsilon_k)_i$ is detailed in M_k.

The general principle for testing the behavior of (2) is to check whether the origin of the coordinate axes belongs to the zonotope (12) (see [22]):

$$\{0\} \in \mathcal{M}(N_k + M_k\upsilon_k) \tag{13}$$

Let us posit $z_k = N_k + M_k\upsilon_k$. The first step of the algorithm consists in checking if $\{0\}$ belongs to the axis-align outer-bounding orthotope $\mathcal{M}^\square(z_k)$, which has the advantage of requiring fewer computations than required for testing (13). It is enough to look separately for the bounds of each variable $(z_k)_i$ and then testing whether $\{0\} \in \mathcal{M}((z_k)_i)$.

The domain $\mathcal{M}((z_k)_i)$ may also be written $\mathcal{M}(e_i^{p\top}(M_k\upsilon_k+ N_k))$ where e_i^p is a canonical vector. Because $\mathcal{M}(w^\top \upsilon) = [-\|w\|_1, \|w\|_1]$, where w is a vector of real values and υ a normalized vector of uncertainties. Because z_k belongs to $\mathcal{M}^\square(z_k)$, it satisfies:

$$\forall i \in \{1, \dots, n\}, |(z_k)_i - e_i^{p\top} N_k| \leq \|e_i^{p\top} M_k\|_1 \tag{14}$$

Nevertheless, except if z_k is scalar or if $\{0\} \notin \mathcal{M}^\square(z_k)$, working on $\mathcal{M}^\square(z_k)$ is less accurate than working on $\mathcal{M}(z_k)$. The membership domain $\mathcal{M}(z_k)$ is a zonotope [20,22] centred on N_k, in other words, a convex domain delimited by couples of parallel hyperplanes. Let us firstly posit $z'_k = z_k - N_k$ and calculate $\mathcal{M}(z'_k)$ centred on the origin instead of $\mathcal{M}(z_k)$. By its very nature, a zonotope is the intersection of strip constraints $\mathcal{S}_i$, written in a general manner: $\mathcal{S}_i(z'_k) = \{z'_k/|\alpha_i^\top z'_k| \leq \beta_i, \alpha_i \in \mathbb{R}^p, \beta_i \in \mathbb{R}^+\}$. This strip constraint can be reformulated as a function of z_k:

$$\mathcal{S}_i(z_k) = \left\{ \begin{array}{l} z_k/ -\beta_i + \alpha_i^\top N_k \leq \alpha_i^\top z_k \leq \beta_i + \alpha_i^\top N_k, \\ \alpha_i \in \mathbb{R}^p, \beta_i \in \mathbb{R}^+ \end{array} \right\} \tag{15}$$

where α_i defines the direction of hyperplanes and β_i the width of the strip. The computation of these values is explained bellow.

Checking (13) can be done by decomposing $\mathcal{M}(z_k)$ into strip constraints: $\mathcal{M}(z_k) = \bigcap_i \mathcal{S}_i(z_k)$. Taking into account (15), test (13) becomes:

$$\bigwedge_i(\{0\} \in \mathcal{S}_i(z_k)) \Leftrightarrow \bigwedge_i(-\beta_i + \alpha_i^\top N_k \leq 0 \leq \beta_i + \alpha_i^\top N_k) \tag{16}$$

If condition (16) is not satisfied, a fault is detected.

Definition 11 *A directional matrix is a matrix composed of canonical vectors e_i^s: $[\,e_{i_1}^s\ \dots\ e_{i_q}^s\,]$. The set of all $(s \times q)$-dimensional directional matrix is denoted $\mathcal{E}_q^s$.*

The membership value set $\mathcal{M}(z_k)$ can be seen as an affine transformation of a normalized orthotope aligned with coordinate axes of $\mathbb{R}^{q_1+hq_2}$ into a zonotope of $\mathbb{R}^p$. Therefore, $(p-1)$-dimensional facets delimiting the zonotope correspond to transformation of some axes aligned hyperplanes of $\mathbb{R}^{q_1+hq_2}$. All the axis aligned hyperplanes are generated by directional matrices $E \in \mathcal{E}_{p-1}^{q_1+hq_2}$. Consequently, the facets of the zonotope are generated by:

$$\mathcal{E}(M_k) = \{E \in \mathcal{E}_{p-1}^{q_1+hq_2}/rank(M_kE) = p-1\} \tag{17}$$

At most, there are $\begin{pmatrix} q_1 + hq_2 \\ p-1 \end{pmatrix}$ strip constraints and two times more facets.

Proposition 12 *All the strip constraints $\mathcal{S}_i(z_k)$ are defined by vectors α_i and scalars β_i satisfying:*

$$\mathcal{P}(M_k) = \left\{ \begin{array}{l} (\alpha_i, \beta_i) \in (\mathbb{R}^p \times \mathbb{R}) \, / \\ \alpha_i^\top M_k E = 0, \beta_i = \|\alpha_i^\top M_k\|_1, E \in \mathcal{E}(M_k) \end{array} \right\} \quad (18)$$

PROOF. If $\mathcal{S}_i(z_k)$ is a strip constraint, all the vectors belonging to a facet generated by $M_k E$, $\forall E \in \mathcal{E}(M_k)$, defined in (17), are perpendicular to the vector α_i. It yields that $\alpha_i^\top M_k E = 0$ if $E \in \mathcal{E}(M_k)$. Moreover, the zonotope $\mathcal{M}(z_k)$ corresponds to the values z_k satisfying all the strip constraints. Therefore, $z_k = M_k v_k + N_k$ has to satisfy (15). Introducing the expression of z_k into (15) leads to $-\beta_i \leq \alpha_i^\top M_k v_k \leq \beta_i$. Because $\mathcal{M}(\alpha_i^\top M_k v_k) = [-\|\alpha_i^\top M_k\|_1, \|\alpha_i^\top M_k\|_1]$, it yields $\beta_i = \|\alpha_i^\top M_k\|_1$.

To summarize, testing (13) is achieved by checking strip constraints (16) defined by (18) with (17). If test fails, it proves that there is a fault. If all the tests have succeeded, the behaviour of system (2) is not suspected.

Let us take the example of a domain $z = Mv$ defined by the following matrix M:

$$M = \begin{bmatrix} 2 & -1 & -1 \\ 1 & 1 & 0 \end{bmatrix}$$

In this case, p is equal to 2 and $dim(v) = 3$. All the $(p-1)$ groups of canonical vectors, i.e. all the canonical vectors e_i^3, have to be considered in order to find the facets:

$$E_1 = \begin{bmatrix} 1 \\ 0 \\ 0 \end{bmatrix}, E_2 = \begin{bmatrix} 0 \\ 1 \\ 0 \end{bmatrix}, E_3 = \begin{bmatrix} 0 \\ 0 \\ 1 \end{bmatrix}$$

The parameters of the strips constraints can be deduced from (18):

$$\alpha_1^T = [1 \ \ -2], \beta_1 = 4$$
$$\alpha_2^T = [1 \ \ 1], \beta_2 = 4$$
$$\alpha_3^T = [0 \ \ 1], \beta_3 = 2$$

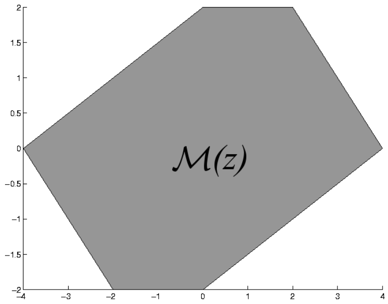

Fig. 1. Resulting membership domain of the example

The strips constraints can be deduced from (15):

$$\mathcal{S}_1(z) = \{z/|[1 \ \ -2]z| \leq 4\}$$
$$\mathcal{S}_2(z) = \{z/|[1 \ \ 1]z| \leq 4\}$$
$$\mathcal{S}_3(z) = \{z/|[0 \ \ 1]z| \leq 2\}$$

Figure 1 illustrates the resulting membership domain $\mathcal{M}(z)$.

The dichotomous results of test (13) may appear somewhat poor. In addition to test (13), it is possible to evaluate the distance separating the origin of the coordinate axes to the closest facet of $\mathcal{M}(z_k)$ instead of just testing (13). In this way, a Boolean decision is combined with a distance to the opposite decision. Instead of directly using the distance from the origin to the closest facet, it seemed more apposite to assess the quotient between this distance and the distance separating the centre of the zonotope and the closest facet to origin. The advantage of this quotient is that it normalizes the result: a distance of 1 when no fault is detected means that the centre of the zonotope corresponds to the origin of the coordinate axes, whereas when a fault is detected, the value 1 means that the origin of the coordinate axes is as far from the closest facet as the centre of the zonotope is from this facet. Moreover, the more this normalized distance tends to zero, the closer the origin of the coordinate axes gets to a facet, in other words, the smaller the distance to the opposite decisions is. In [14], it has been shown that this normalized distance is given by:

$$d = \frac{min(|\alpha_{i^*}^\top N_k - \beta_{i^*}|, |\alpha_{i^*}^\top N_k + \beta_{i^*}|)}{|\beta_{i^*}|}, \quad (19)$$
$$i^* = arg\left(\underset{(\alpha_i,\beta_i)\in\mathcal{P}(M_k)}{min} \left(\frac{\beta_i}{\alpha_i^\top N_k} \right) \right)$$

The different variables appearing in (19) are drawn in figure 2.

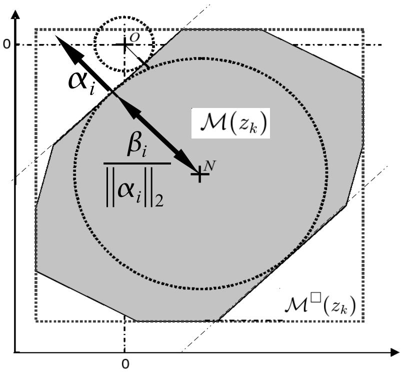

Fig. 2. Principle of distance computation

5 Example

This example is based on a real lab application. It is composed of two identical stacked water tanks, with a section equal to S. The upper tank, corresponding to index 1, fills the lower tank with index 2. The external input flows, controlled by Kammer valves, are denoted by ϕ_{i_1} and ϕ_{i_2}. The output flows are ϕ_{o_1} and ϕ_{o_2}. ϕ_{o_1} flows into the lower tank. The water levels are l_1 and l_2. Each tank output flow ϕ_{o_i} is proportional (parameter α) to the water level l_i. A detailed model of the normal behaviour of this application has been presented in [15]. A state space representation of the water tank system is given by:

$$\begin{cases} \frac{d}{dt}\begin{bmatrix} l_1 \\ l_2 \end{bmatrix} & = \frac{\alpha}{S}\begin{bmatrix} -(1+\rho\upsilon_1) & 0 \\ 1+\rho\upsilon_1 & -(1+\rho\upsilon_2) \end{bmatrix}\begin{bmatrix} l_1 \\ l_2 \end{bmatrix} \\ & \ldots + \frac{1}{S}\begin{bmatrix} 1 & 0 \\ 0 & 1 \end{bmatrix}\begin{bmatrix} \tilde{\phi}_{i_1} \\ \tilde{\phi}_{i_2} \end{bmatrix} \\ \begin{bmatrix} \tilde{l}_1 \\ \tilde{l}_2 \end{bmatrix} & = \begin{bmatrix} l_1 \\ l_2 \end{bmatrix} + \lambda \begin{bmatrix} \epsilon_1 \\ \epsilon_2 \end{bmatrix} \end{cases}$$

where $S = 7.10^{-2}m^2$, $\alpha = 7.10^{-3}m^2s^{-1}$, $\rho = 60\%$, $\lambda = 4$mm and υ_1, υ_2, ϵ_1, ϵ_2 are time-varying uncertain normalized variables. Variables υ_1 and υ_2 model the uncertainties in the output restriction due to the formation of air bubbles. Actual parameter α varies up from $\pm 60\%$ of its nominal values. Variables ϵ_1 and ϵ_2 stand for measurement noises that can get up to ± 4mm. Thanks to the formulae given in [1], this state space model has been transformed into a discrete-time model with a 1 second sample time:

$$\begin{cases} \begin{bmatrix} l_{1,k+1} \\ l_{2,k+1} \end{bmatrix} & = (A_0 + A_1\upsilon_{1,k} + A_2\upsilon_{2,k})\begin{bmatrix} l_{1,k} \\ l_{2,k} \end{bmatrix} \\ & \ldots + (B_0 + B_1\upsilon_{1,k} + B_2\upsilon_{2,k})\begin{bmatrix} \tilde{\phi}_{i_1,k} \\ \tilde{\phi}_{i_2,k} \end{bmatrix} \\ \begin{bmatrix} \tilde{l}_{1,k} \\ \tilde{l}_{2,k} \end{bmatrix} & = \begin{bmatrix} l_{1,k} \\ l_{2,k} \end{bmatrix} + \lambda \begin{bmatrix} \epsilon_{1,k} \\ \epsilon_{2,k} \end{bmatrix} \end{cases} \quad (20)$$

with

$$A_0 = \begin{bmatrix} 0.9048 & 0 \\ 0.0905 & 0.9048 \end{bmatrix}, A_1 = \begin{bmatrix} -0.0905\rho & 0 \\ 0.086\rho & 0 \end{bmatrix}$$

$$A_2 = \begin{bmatrix} 0 & 0 \\ -0.0045\rho & -0.0905\rho \end{bmatrix}, B_0 = \begin{bmatrix} 13.5947 & 0 \\ 0.6684 & 13.5947 \end{bmatrix}$$

$$B_1 = \begin{bmatrix} 0.6684\rho & 0 \\ 0.6463\rho & 0 \end{bmatrix}, B_2 = \begin{bmatrix} 0 & 0 \\ -0.0221\rho & -0.6684\rho \end{bmatrix}$$

Simulations last 1400s. Figure 3 represents the values that have been used for bounded variables $\upsilon_{1,k}$, $\upsilon_{2,k}$, $\epsilon_{1,k}$ and $\epsilon_{2,k}$. External input flows have been drawn on figure 4.

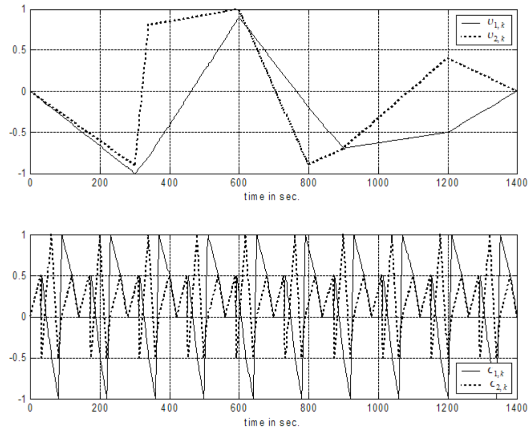

Fig. 3. Variations of uncertain variables

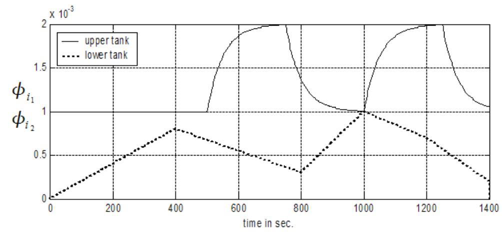

Fig. 4. External input water flows in $m^3.s^{-1}$ (normal behaviour)

In simulations, a leak in the upper tank, starting at 600s, has been simulated. It has been modelled by an additional output flow in the upper tank, which does not flow into the lower tank (see figure 5).

The simulated water levels when normal behaviour and when the leak occurs, are represented in figure 6.

In order to appreciate the interest of the set-membership approach, the deterministic parity relation approach, presented in (Massoumnia and Van Der Velde, 1988), has been firstly applied. Only the deterministic part of (20)

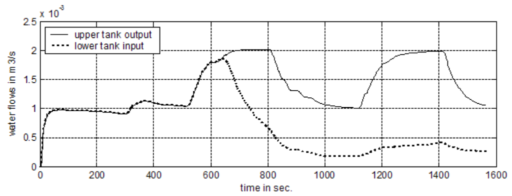

Fig. 5. Leak in $\mathrm{m}^3.\mathrm{s}^{-1}$

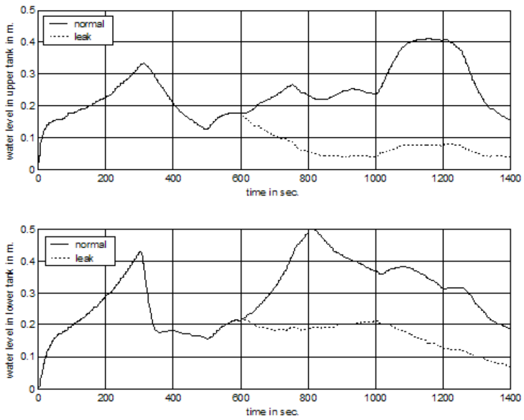

Fig. 6. Water levels in the 2 tanks (normal behaviour and leak)

is considered: uncertain variables are neglected. Outputs are stacked over an horizon of 2 in order to be able to cancel the unknown variables and to generate as many parity relations as the number of outputs:

$$\begin{bmatrix} \tilde{y}_k \\ \tilde{y}_{k+1} \end{bmatrix} = \begin{bmatrix} I_2 \\ A_0 \end{bmatrix} \begin{bmatrix} l_{1,k} \\ l_{2,k} \end{bmatrix} + \begin{bmatrix} 0 \\ B_0 \end{bmatrix} \begin{bmatrix} \tilde{\phi}_{i_1,k} \\ \tilde{\phi}_{i_2,k} \end{bmatrix}$$

A matrix Ω_0 is chosen so that it cancels term in x_k. The expression of residuals comes directly from this cancellation:

$$r_{k+1} = \Omega_0 \begin{bmatrix} \tilde{y}_k \\ \tilde{y}_{k+1} \end{bmatrix} - \Omega_0 \begin{bmatrix} 0 \\ B_0 \end{bmatrix} \tilde{u}_k,\ \Omega_0 \begin{bmatrix} I_2 \\ A_0 \end{bmatrix} = 0$$

The numerical result is given by:

$$r_{k+1} = \begin{bmatrix} -0.0151 & 0.667 & 0.0904 & -0.7371 \\ -0.6713 & -0.0527 & 0.7361 & 0.0583 \end{bmatrix} \begin{bmatrix} \tilde{l}_{1,k} \\ \tilde{l}_{2,k} \\ \tilde{l}_{1,k+1} \\ \tilde{l}_{2,k+1} \end{bmatrix}$$

$$\ldots + \begin{bmatrix} -0.7362 & 10.021 \\ -10.046 & -0.792 \end{bmatrix} \begin{bmatrix} \tilde{\phi}_{i_1,k} \\ \tilde{\phi}_{i_2,k} \end{bmatrix}$$

In spite of deterministic approach neglects uncertainties in models, thresholds have to be fixed a posteriori and experimentally because instead of residuals to be null, they are only "almost null". In the presented example, the thresholds have been fixed at ± 0.015 (imposed by time 300s.) for the first residuals and at ± 0.017 (imposed by time 330s.) for the second one according to normal behavior simulation. Thresholds correspond to the lower and upper limits of the plots. Figure 7 shows that the leak is not detected with this approach.

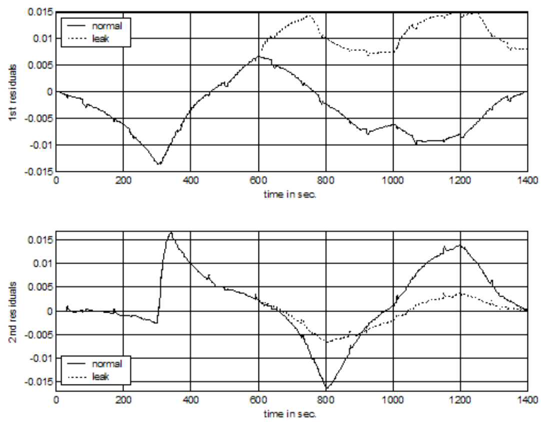

Fig. 7. Detection results of deterministic parity relations

Let's now design uncertain parity relations. According to the method depicted in section 3, the horizon h remains the same as the horizon required for the deterministic approach ($h = 2$) because the system is regularly observable. The matrix $\mathcal{O}_2(\upsilon_{1,k}, \upsilon_{2,k})$, obtained from the discrete-time state space model (20), is indeed regular in the uncertainties because its rank remains the same whatever the values of bounded variables are:

$$\mathcal{O}_2(\upsilon_{1,k}, \upsilon_{2,k}) = \ldots$$

$$\begin{bmatrix} 1 & 0 \\ 0 & 1 \\ 0.9048 - 0.0543\upsilon_{1,k} & 0 \\ 0.0905 + 0.0516\upsilon_{1,k} - 0.0027\upsilon_{2,k} & 0.9048 - 0.0543\upsilon_{2,k} \end{bmatrix}$$

Then, the matrix $\Omega(\upsilon_{1,k}, \upsilon_{2,k})$ cancelling $\mathcal{O}_2(\upsilon_{1,k}, \upsilon_{2,k})$ is obtained thanks to algorithm proposed in section 3, except for Ω_o, which is the same as the matrix Ω computed in the deterministic approach:

$$\Omega(\upsilon_{1,k}, \upsilon_{2,k}) = \begin{bmatrix} \Omega_{11} & \Omega_{12} & \Omega_{13} & \Omega_{14} \\ \Omega_{21} & \Omega_{22} & \Omega_{23} & \Omega_{24} \end{bmatrix}$$

$$\begin{cases} \Omega_{11} = -0.0151 + 0.0429\upsilon_{1,k} - 0.002\upsilon_{2,k} \\ \Omega_{12} = 0.667 - 0.04\upsilon_{2,k} \\ \Omega_{13} = 0.0904, \Omega_{14} = -0.7371 \\ \Omega_{21} = -0.6713 + 0.037\upsilon_{1,k} + 0.0002\upsilon_{2,k} \\ \Omega_{22} = -0.0527 + 0.0032\upsilon_{2,k} \\ \Omega_{23} = 0.7361, \Omega_{24} = 0.0583 \end{cases}$$

Because $\Omega(\upsilon_{1,k}, \upsilon_{2,k})$ is already affine with respect to the uncertainties, it leads directly to the following uncertain parity relation, where uncertain variables have been collected:

$$r_{k+1} = \begin{bmatrix} R_1 \\ R_2 \end{bmatrix} + \begin{bmatrix} U_{11} & U_{12} \\ U_{21} & U_{22} \end{bmatrix} \begin{bmatrix} \upsilon_{1,k} \\ \upsilon_{2,k} \end{bmatrix} \dots$$

$$+ \begin{bmatrix} 0.0001 & -0.0027 & -0.0004 & 0.0029 \\ 0.0027 & 0.0002 & -0.0029 & -0.0002 \end{bmatrix} \begin{bmatrix} \epsilon_{1,k} \\ \epsilon_{2,k} \\ \epsilon_{1,k+1} \\ \epsilon_{2,k+2} \end{bmatrix}$$

$$\begin{cases} R_1 & = -0.015\tilde{l}_{1,k} + 0.667\tilde{l}_{2,k} + 0.09\tilde{l}_{1,k+1} \\ & \dots - 0.737\tilde{l}_{2,k+1} - 0.7362\tilde{\phi}_{i_1,k} + 10.021\tilde{\phi}_{i_2,k} \\ R_2 & = -0.671\tilde{l}_{1,k} - 0.053\tilde{l}_{2,k} + 0.736\tilde{l}_{1,k+1} \\ & \dots + 0.058\tilde{l}_{2,k+1} - 10.046\tilde{\phi}_{i_1,k} - 0.792\tilde{\phi}_{i_2,k} \\ U_{11} & = 0.043\tilde{l}_{1,k} + 0.322\tilde{\phi}_{i_1,k} \\ U_{12} & = -0.002\tilde{l}_{1,k} - 0.04\tilde{l}_{2,k} - 0.0098\tilde{\phi}_{i_1,k} - 0.296\tilde{\phi}_{i_2,k} \\ U_{21} & = 0.037\tilde{l}_{1,k} + 0.273\tilde{\phi}_{i_1,k} \\ U_{22} & = 0.0002\tilde{l}_{1,k} + 0.003\tilde{l}_{2,k} + 0.0008\tilde{\phi}_{i_1,k} + 0.0234\tilde{\phi}_{i_2,k} \end{cases}$$

At each sample time, this final numerical expression is recomputed taking into account the updated known data about water levels and input flows. Then, the consistency with the model is checked by computing and testing the constraints (16).

Finally, the distance (19) is computed at each sample time. As an illustration, considered sample 200. The following strip constraints depicting $\mathcal{M}(r_{200})$ have been found:

$$\begin{aligned} \mathcal{S}_1 &: -0.0218 \leq \ \ 0.6522r_{1,k} - 0.7580r_{2,k} \leq 0.0113 \\ \mathcal{S}_2 &: -0.0210 \leq -0.0788r_{1,k} - 0.9969r_{2,k} \leq 0.0089 \\ \mathcal{S}_3 &: -0.0287 \leq \ \ 0.9997r_{1,k} - 0.0225r_{2,k} \leq 0.0266 \\ \mathcal{S}_4 &: -0.0210 \leq -0.0788r_{1,k} - 0.9969r_{2,k} \leq 0.0089 \\ \mathcal{S}_5 &: -0.0284 \leq \ \ 0.9925r_{1,k} - 0.1219r_{2,k} \leq 0.0251 \end{aligned}$$

The membership domain has been drawn in figure 8. Because origin belongs to the membership domain, there is no alarm at this time. The distance is equal to 0.5928: it is far from the closest border i.e. far from alarm thresholds.

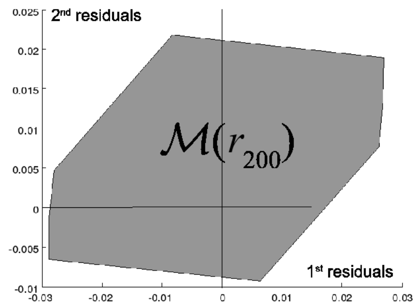

Fig. 8. Membership value set of residuals at sample 200

In order to summarize results with only one curve, these two results have been combined into an unique indicator, which corresponds to the distance to the closest facet multiplied by 1 in case of alarm and by -1 elsewhere [4]. It is drawn on figure 9. When the closest facet proximity exceeds 0, it means that a fault has been detected.

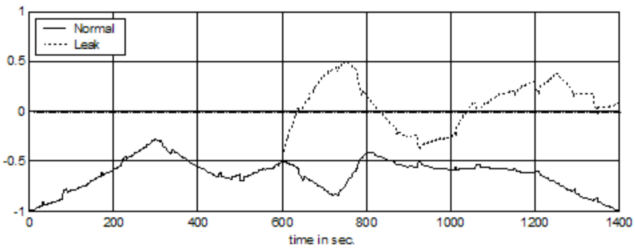

Fig. 9. Detection indicators based on uncertain parity relations

Figure 9 shows the detection results of the uncertain parity relation when a leak is simulated from time 600s. The leak is detected from sample 620 to 820 and from 1020 to 1400 whereas it is not detected with deterministic parity relations (figure 7).

6 Conclusion

Uncertain parity relations are an interesting alternative to the state-estimation approaches that require integration with respect to the time and therefore set the problem of wrapping effect, which is often solved by degrading the guarantee property. The proposed parity relation design method apply to any uncertain linear system assuming that it is regularly observable. Uncertain parity relations are powerful tools to handle uncertain dynamic systems where multiplicative uncertainties are predominant. The deterministic approach becomes indeed imprecise because the a posteriori thresholds offsetting the neglected uncertain part of the deterministic model becomes not conservative enough. Although the uncertain

[4] Because on one hand a distance is positive and on the other hand the value set membership is Boolean, distance and membership can be merged without loss of information.

parity relations require some approximation due to linearizations, they require very little computation times: this approach comes down computing and checking linear inequalities at each sample time. Uncertain parity relation not only provides boolean detection result, but it also provides an indicator representing the distance to the opposite decision. The approximations required by the design of uncertain parity relations, can be offset by an a posteriori retuning of the additive uncertain variables. The 2 water tanks application example has shown that, in some situations, uncertain parity relations lead to more precise decisions than deterministic parity relations.

Acknowledgements

Authors would particularly like to thank the reviewers for their help and for their constructive remarks.

References

[1] 0. Adrot and S. Ploix. Fault detection based on set-membership inversion. In *SAFEPROCESS'2006*, Beijing, China, 2006.

[2] O. Adrot and J. M. Flaus. Trajectory computation of a dynamic uncertain syste. In *IEEE Conference on Decision and Control*, Hawaï, USA, 2003.

[3] J. Armengol, L. Travé-massuyès, J. Vehi, and J. L. de la Rosa. A survey on interval model simulators and their properties related to fault detection. In *14th IFAC World Congress*, Beijing, China, 1999.

[4] E. Y. Chow and A. S. Willsky. Analytical redundancy and the design of robust failure detection systems. *IEEE transactions on Automatic Control*, 29:603–614, 1984.

[5] J. De Kleer and B. C. Williams. Diagnosing multiple faults. *Artificial Intelligence*, 32:97–130, 1987.

[6] O. Didrit. *Analyse par intervalles pour l'automatique; résolution globale et garantie de problèmes non-linéaires en robotique et en commande robuste.* PhD thesis, Université Paris XI, 1997.

[7] E. R. Hansen. *Global optimization using interval analysis.* Marcel Dekker, New-York, U.S.A, 1992.

[8] D. T. Horak and B. H. Allison. Failure detection and isolation methodology. In *American Control Conference*, San Diego, California, U.S.A, 1990.

[9] M. M. Massoumnia and W. E. Van Der Velde. Generating parity relations for detecting and identifying control system component failures. *Journal of guidance, control and dynamics*, 11(1):60–65, 1988.

[10] M. Milanese, J. Norton, H. Piet Lahanier, and E. Walter, editors. *Bounding approaches to system identification.* Plenum Press, New-York, U.S.A. and London, U.K., 1996.

[11] J. Norton. Identification and application of bounded-parameter models. *Automatica*, 23(4):497–508, 1987.

[12] M. Nyberg and M. Krysander. Combining ai, fdi, and statistical hypothesis-testing in a framework for diagnosis. In *IFAC Safeprocess'03*, Washington, U.S.A., 2003.

[13] R. Patton. Robust model-based fault diagnosis: the state of the art. In *SAFEPROCESS'94*, Espoo, Finland, 1994.

[14] S. Ploix, O. Adrot, and J. Ragot. Bounding approach to the diagnosis of a class of uncertain static systems. In *SAFEPROCESS'2000*, Budapest, Hungary, 2000.

[15] S. Ploix, S. Touaf, and J. M. Flaus. A logical framework for isolation in fault diagnosis. In *SAFEPROCESS'2003*, Washington D.C., U.S.A., 2003.

[16] V. Puig, J. Quevedo, T. Escobet, and S. De Las Heras. Passive robust fault detection approaches using interval models. In *15th Triennal IFAC World Congress*, Barcelona, Spain, 2002.

[17] R. Reiter. A theory of diagnosis from first principles. *Artificial Intelligence*, 32:57–95, 1987.

[18] F. C. Schweppe. *Uncertain dynamic systems.* Prentice Hall, Englewood Cliffs, N. J., U.S.A., 1973.

[19] M. Staroswiecki, V. Cocquempot, and J. P. Cassar. Observer based and parity space approaches for failure detection and identification. In *IMACS-IFAC International Symposium*, Lille, France, 1991.

[20] A. Vicino and G. Zappa. Adaptative approximation of uncertainty sets for linear regression models. In M. Milanese, J. Norton, H. Piet-Lahanier, and E. Walter, editors, *Bounding approaches to system identification*, pages 159–181. Plenum Press, New-York, U.S.A. and London, U.K., 1996.

[21] E. Walter and H. Piet-Lahanier. Exact and recursive description of feasible parameter set for bounded error models. In *26th IEEE Conference on Decision and Control*, Los Angeles, U.S.A., 1987.

[22] G. M. Ziegler. *Lectures on Polytopes.* Graduate Texts in Mathematics 152. Springer-Verlag, New York, U.S.A, 1998.

7 Biography

S. Ploix is Assistant Professor at the INP Grenoble. After an engineer degree in Mechanics and Electricity, he obtained in 1998, a PhD from the INP Lorraine in Control engineering and Signal processing. He is a specialist in supervision, monitoring and diagnosis. He has developed tools based on set-membership and logical reasoning for the diagnosis of complex system that take into account human factor. He is involved in different application fields such as supervision of distributed industrial plants, diagnosis of human skills and iterative diagnosis tool for companies.

O. Adrot is Assistant Professor at the Polytech'Grenoble (Université Joseph Fourier). In 1995 he obtained an engineer degree in Electrical Engineering from the Ecole Supérieure Atlantique d'Ingénieurs en Génie Electrique. In 2000 he obtained a PhD from the Institut National Polytechnique de Lorraine in Control engineering and Signal processing. He has worked on set-membership approaches for uncertain modelling, fault detection and safety analysis.